Chapter 5

Relationship of cerebrospinal fluid markers with [^{11}C]PIB and [^{18}F]FDDNP binding

Nelleke Tolboom, Wiesje M. van der Flier, Maqsood Yaqub, Ronald Boellaard, Nicolaas A. Verwey, Marinus A. Blankenstein, Albert D. Windhorst, Philip Scheltens, Adriaan A. Lammertsma, Bart N.M. van Berckel

Journal of Nuclear Medicine 2009;50:1464-70.

Abstract

Objective: The purpose of this study was to investigate potential relationships between cerebrospinal fluid (CSF) measurements of beta-amyloid 1–42 (Aβ42) and total tau with [^{11}C]PIB and [^{18}F]FDDNP binding as measured using positron emission tomography (PET).

Methods: A total of 37 subjects were included, consisting of 15 patients with Alzheimer's disease (AD), 12 patients with mild cognitive impairment (MCI) and 10 healthy controls. All subjects underwent a lumbar puncture and PET scanning using both [^{11}C]PIB and [^{18}F]FDDNP. For both PET tracers, parametric images of binding potential (BP_{ND}) were generated. Potential associations of CSF levels of Aβ42 and tau with [^{11}C]PIB and [^{18}F]FDDNP binding were assessed using Pearson's correlations coefficients and linear regression analyses.

Results: For both global [^{11}C]PIB and [^{18}F]FDDNP binding, significant correlations with CSF levels of Aβ42 ($r=-0.72$ and $r=-0.37$) and tau ($r=0.58$ and $r=0.56$) were found across groups (all $p<0.001$, except $p<0.05$ for correlation between [^{18}F]FDDNP and Aβ42). Linear regression analyses showed that, adjusted for regional volume, age, sex and diagnosis, global [^{11}C]PIB uptake had an inverse association with Aβ42 CSF levels (standardised $\beta=-0.50$, $p<0.001$), whilst there was a positive association between global [^{18}F]FDDNP binding and tau CSF levels (standardised $\beta=0.62$, $p<0.01$).

Conclusions: The good agreement between these two different types of biomarkers (i.e. CSF and PET) provides converging evidence for their validity. The inverse association between [^{11}C]PIB and CSF Aβ42 confirms that [^{11}C]PIB measures amyloid load in the brain. The positive association between [^{18}F]FDDNP and CSF tau suggests that at least part of the specific signal of [^{18}F]FDDNP in AD patients is due to tangle formation.

Introduction

At present, there are two promising methods for *in vivo* assessment of the extent of Alzheimer's disease (AD) pathology. One is the use of cerebrospinal fluid (CSF) biomarkers of beta-amyloid-1-42 (Aβ42) and tau, the other imaging of neuropathology associated with AD using positron emission tomography (PET) and [^{11}C]PIB (Pittsburgh Compound B) or [^{18}F]FDDNP (2-(1-{6-[(2-[F-18]fluoroethyl)(methyl)amino]-2-naphthyl}ethylidene) malononitrile) *(1)*,*(2)*. Biochemical changes in CSF (decrease of Aβ42 and increase of tau) are thought to indirectly reflect the presence of AD pathology (3). Imaging using either [^{11}C]PIB or [^{18}F]FDDNP is thought to provide a more direct reflection of AD pathology in the brain. [^{11}C]PIB was designed to measure the amount of fibrillar Aβ deposits (*4*,*5*) which has been confirmed by a post-mortem study in AD *(6)*. [^{18}F]FDDNP has been reported to label not only amyloid but also neurofibrillary tangles which co-localised with conventional immmunohistochemistry measures (*2*,*7*) and neuropathologically in an AD patient *(2)*. Compared to [^{11}C]PIB, however, limited information is available on *in vivo* [^{18}F]FDDNP binding in AD patients.

Although it is generally accepted that both types of markers (i.e. CSF and PET) reflect amyloid and/or tau load, the relationship between these two types of biomarkers has not been studied extensively. Only a few studies have investigated the relationship between [^{11}C]PIB and CSF measurements. Studies were performed in groups mainly consisting of healthy controls (*8*,*9*) or patients with mild cognitive impairment (MCI) (*10*,*11*) and recently in a group consisting solely of AD patients *(12)*. In these studies an inverse relationship between [^{11}C]PIB and CSF Aβ42 levels was found, but either no *(8)* or only a modest *(10)* relationship between [^{11}C]PIB and CSF tau levels. No studies have been published describing the relationship between [^{18}F]FDDNP binding and CSF biomarker levels.

In our previous study, paired [^{11}C]PIB and [^{18}F]FDDNP studies were performed in AD patients, MCI patients and healthy controls *(13)*. Both tracers were able to distinguish AD patients from healthy controls at a group level, but specific binding of [^{11}C]PIB in AD patients was substantially higher than that of [^{18}F]FDDNP. The moderate correlation between global cortical binding of both tracers suggested that they measured related, but different aspects of the neuropathology associated with AD. The purpose of the present study was to investigate potential relationships between CSF measurements of Aβ42 and tau, and PET measurements using [^{11}C]PIB and [^{18}F]FDDNP.

Subjects and Methods

Subjects

15 AD patients, 12 patients with amnestic MCI and 10 healthy controls, for which paired [^{11}C]PIB, [^{18}F]FDDNP and CSF data were available, were included *(13)*. Global and regional [^{11}C]PIB and [^{18}F]FDDNP binding of an overlapping sample has been presented before *(13)*. All patients received a standard dementia screening that included medical history, physical and

neurological examinations, laboratory tests, brain magnetic resonance imaging (MRI), and extensive neuropsychological testing. Clinical diagnosis was established by consensus in a multidisciplinary team, without knowledge of PET and CSF data. All AD patients met NINCDS-ADRDA criteria for "probable AD" *(14)*. MCI patients met Petersen criteria based on subjective and objective cognitive impairment, predominantly affecting memory, in the absence of dementia or significant functional loss *(15)*. Control subjects were recruited through advertisements in newspapers and underwent the same diagnostic procedures. Exclusion criteria were history of major psychiatric or neurological (other than AD) illness and use of non-steroidal anti-inflammatory drugs (NSAIDS), as these have been reported to compete with [^{18}F]FDDNP for binding to Aβ fibrils *in vitro* and to Aβ plaques *ex vivo (16)*. Additional exclusion criteria for controls were: subjective memory complaints or clinically significant abnormalities on the MRI scan (as determined by a neuroradiologist). Written informed consent was obtained from all subjects after a complete written and verbal description of the study. The study was approved by the Medical Ethics Review Committee of the VU University Medical Centre Amsterdam.

Positron emission tomography

PET scans were performed on an ECAT EXACT HR+ scanner (Siemens/CTI, Knoxville, USA), equipped with a neuro-insert. This scanner enables the acquisition of 63 transaxial planes over a 15.5 cm axial FOV, thus allowing the whole brain to be imaged in a single bed position. The properties of this scanner have been reported previously *(17)*. All subjects received a venous cannula for tracer injection. Patient motion was restricted by the use of a head holder and monitored using laser beams. First, a 10 minutes transmission scan was performed in 2D acquisition mode using three retractable rotating line sources to correct the subsequent emission scan for photon attenuation. Next, a dynamic emission scan in 3D acquisition mode was started simultaneously with the intravenous injection of 354±74 MBq [^{11}C]PIB with a specific activity (SA) of 43±25 GBq/μmol using an infusion pump (Med-Rad, Beek, the Netherlands) followed by a flush of saline, at a rate of 0.8 mL/sec for the first 5 mL and 2.0 mL/sec thereafter. Radiolabeled [^{11}C]PIB was synthesised according to a modification *(18)* of the procedure described by Wilson et al *(19)*. The dynamic emission scan consisted of 23 frames with progressive increase in frame duration (1x15, 3x5, 3x10, 2x30, 3x60, 2x150, 2x300, 7x600 s) for a total duration of 90 minutes. Finally, after a resting period of at least 1 hour to allow for decay of ^{11}C (i.e. about 2.5 hours after the administration of [^{11}C]PIB), exactly the same procedure was repeated, but now using an injection of 178±14 MBq [^{18}F]FDDNP *(20)* with an SA of 76±49GBq/μmol.

Magnetic resonance imaging

All subjects underwent a structural MRI scan using a Siemens 1.5 T Sonata scanner (Siemens Medical Solutions, Erlangen, Germany). The scan protocol included a coronal T1-weighted 3D MPRAGE (magnetization prepared rapid acquisition gradient echo; slice thickness 1.5 mm, 160 slices; matrix size 256x256; voxel size 1x1x1.5 mm; echo time=3.97 ms; repetition time=2700

ms; inversion time=950 ms; flip angle 8°), which was used for co-registration and region of interest (ROI) definition.

Image analysis

All PET sinograms were corrected for dead time, tissue attenuation using the transmission scan, decay, scatter and randoms, and were reconstructed using a standard filtered back projection algorithm and a Hanning filter with a cut-off at 0.5 times the Nyquist frequency. A zoom factor of 2 and a matrix size of 256×256×63 were used, resulting in a voxel size of 1.2×1.2×2.4 mm and a spatial resolution of approximately 7mm full-width at half-maximum at the centre of the field of view.

MRI images were aligned to corresponding PET images using a mutual information algorithm *(21)*. Data were further analysed using PVE lab, a software program that uses a previously validated probability-map of 35 delineated ROIs *(22)*. No correction for partial volume effects was applied to the PET data.

ROIs were projected onto [^{11}C]PIB and [^{18}F]FDDNP parametric images of binding potential (BP_{ND}). These parametric images were generated by applying a basis function implementation of the "two-step" simplified reference tissue model with cerebellar grey matter as reference tissue (RPM2) *(23)* to the full dynamic 90 minutes PET data. Recently, RPM2 has been identified as the quantitative method of choice for both tracers (*24*,*25*). BP_{ND} is a quantitative measure of specific binding, reflecting the concentration of specifically bound tracer relative to the concentration of free and non-specifically bound tracer in tissue under equilibrium conditions *(26)*. All ROIs, including cerebellum, and their corresponding grey matter volumes were obtained using PVE lab *(22)*. For regional analyses, BP_{ND} of frontal (volume weighted average of orbital frontal, medial inferior frontal and superior frontal), parietal and temporal (volume weighted average of superior temporal and medial inferior temporal) cortex and medial temporal lobe (MTL) (volume weighted average of enthorinal cortex and hippocampus) and posterior cingulate was used. In addition, a global cortical ROI was defined, based on the volume weighted average of all aforementioned regions. Cerebellar grey matter was chosen as reference tissue because of its (histopathological) lack of Congo red and thioflavin-S–positive plaques (*27*,*28*).

Cerebrospinal fluid

CSF was obtained by lumbar puncture (LP) between L3/L4 or L4/L5 intervertebral spaces, using a 25-gauge needle, and collected in 10 mL polypropylene tubes. Within 2 hours, CSF samples were centrifuged at 1800 g for 10 minutes at 4 °C. A small amount of CSF was used for routine analysis, including total cells (leucocytes and erythrocytes), total protein and glucose. CSF was aliquoted in polypropylene tubes of 0.5 or 1 mL, and stored at −80 °C until further analysis. CSF Aβ42 and tau were measured with Innotest (Innogenetics, Ghent, Belgium) sandwich ELISA as described previously *(29)*. As the manufacturer does not supply control data, performance of the assays was monitored using pools of surplus CSF specimens. In the study period multiple specimens with various concentrations, which were included in 7–18 runs, were used for this

purpose. The mean coefficients of variation (±SD) obtained were 11.3±4.9% for Aβ42 and 9.3±1.5% for tau. Median time from LP to PET was 3 months (interquartile range 6 months). Five subjects (2 AD patients, 1 MCI patient and 2 controls) received their LP more than 12 months apart from (before) the PET scan. After exclusion of these subjects median time from LP to PET was 2.5 months.

Statistical analysis

Data are presented as mean±SD, unless otherwise stated. As CSF biomarker levels were not normally distributed, data were log-transformed. Frequency distributions for sex were compared with Chi-squared tests. For continuous measures, differences between groups were assessed using analysis of variance (ANOVA) with post-hoc least significant difference (LSD) tests and age as covariate.

For assessment of relationships between CSF and BP_{ND} data, first Pearson's correlations were calculated across the entire group. Next, linear regression analyses were performed to adjust for potential confounders using CSF biomarkers as independent and global and regional BP_{ND} as dependent variable. Separate analyses were performed for [^{11}C]PIB and [^{18}F]FDDNP. In the first model, the relationship of each CSF biomarker with both PET tracers was adjusted for grey matter ROI volume. In the second model, analyses were additionally adjusted for age, sex and diagnosis (using dummy variables). In the third model, CSF biomarkers were entered simultaneously, together with the same covariates. This analysis was repeated after exclusion of the 5 subjects with long intervals between LP and PET. Standardised β's are reported to allow comparison of effect sizes. A p value below 0.05 was considered significant.

Results

Demographic and clinical data by patient group are presented in Table 1. The three groups were similar with respect to sex. AD patients tended to be younger than MCI patients and controls. AD patients had lower MMSE scores than control subjects and MCI patients (both $p<0.001$). Group differences were found for CSF levels of Aβ42 and tau ($p\leq0.001$). In addition, groups differed with respect to global cortical [^{11}C]PIB BP_{ND} ($p<0.001$). Only a trend was seen for global cortical [^{18}F]FDDNP BP_{ND} ($p<0.10$). Figure 1 shows parametric [^{11}C]PIB and [^{18}F]FDDNP BP_{ND} images of a typical AD patient and a healthy control.

Table 2 lists Pearson's correlations between Aβ42 and tau levels in CSF and global and regional tracer BP_{ND} across all subjects. Lower Aβ42 and higher tau levels were associated with higher global [^{11}C]PIB binding (Figure 2). This was due to higher binding in all cortical regions investigated for Aβ42 and in all, except MTL, for tau. Furthermore, lower Aβ42 and higher tau levels were associated with higher global [^{18}F]FDDNP binding (Figure 3). In this case, lower CSF Aβ42 was associated with higher uptake in frontal and parietal cortex, but there were no correlations with other brain regions investigated. Higher CSF levels of tau were associated with higher uptake in all regions, except MTL.

Table 1: Demographic and clinical characteristics of the three diagnostic groups.

Variable	Controls	MCI	AD
N	10	12	15
Age, year#	70±6	68±9	63±7
Sex, f/m	3/7	2/10	6/9
MMSE**	29±1	28±2	24±2[a, b]
Aβ1–42 (pg/mL)**	886±244	623±165 b	507±78[b]
Tau (pg/mL)**	264±104	431±269	752±371[b, c]
[^{11}C]PIB BP_{ND}	BP_{ND}	BP_{ND}	BP_{ND}
Global**	0.18±0.30	0.33±0.37	0.86±0.12[a, b]
Frontal	0.22±0.37	0.37±0.42	0.93±0.1[a, b]
Medial temporal	0.08±0.08	0.07±0.06	0.15±0.09[c, d]
Temporal	0.16±0.27	0.31±0.34	0.79±0.11[a, b]
Posterior cingulate	0.17±0.22	0.37±0.38	0.84±0.41[a, b]
Parietal	0.17±0.30	0.34±0.21	0.96±0.20[a, b]
[^{18}F]FDDNP BP_{ND}	BP_{ND}	BP_{ND}	BP_{ND}
Global#	0.06±0.03	0.08±0.05	0.09±0.02
Frontal#	0.05±0.04	0.09±0.06	0.09±0.02
Medial temporal	0.12±0.04	0.13±0.05	0.14±0.05
Temporal	0.07±0.03	0.10±0.05	0.10±0.03
Posterior cingulate	0.04±0.01	0.07±0.02	0.06±0.01
Parietal#	0.02±0.04	0.04±0.04	0.06±0.03

Data are presented as mean ± SD, where appropriate.
MCI, mild cognitive impairment; AD, Alzheimer's disease; f, female; m, male; MMSE, mini-mental-state examination; Aβ1–42, beta-amyloid; BP_{ND}, binding potential.
Note that raw values are shown for CSF biomarkers (pg/mL), but that log-transformed values were used for statistical analysis.
Analysis of variance (ANOVA) with age as covariate:
#) $p < 0.10$
*) $p < 0.05$
**) $p \leq 0.001$
Post-hoc LSD-tests:
a) $p \leq 0.001$ compared to MCI
b) $p \leq 0.001$ compared to controls
c) $p < 0.05$ compared to MCI
d) $p < 0.05$ compared to controls

Next, linear regression analyses were performed to adjust for potential confounders. After adjustment for grey matter ROI volume (model 1), associations were observed between both CSF markers (i.e. low CSF Aβ42 and high CSF tau) and increased global and regional [^{11}C]PIB binding (Table 3). For [^{18}F]FDDNP binding, associations were found between low CSF Aβ42 and increased global, frontal and parietal binding with a trend for temporal binding. In addition, associations were found for high CSF tau and increased [^{18}F]FDDNP binding in all regions, except for MTL were this association displayed a trend (standardised $\beta=0.34$, $p < 0.10$).
After additionally adjusting for age, sex and diagnosis (model 2), an association was observed between CSF Aβ42 and global, frontal, temporal and posterior cingulate [^{11}C]PIB binding, but there was no such association between CSF tau and global or regional [^{11}C]PIB binding. For [^{18}F]FDDNP binding the opposite pattern was observed, i.e. a positive association with CSF levels of tau, but no association with CSF levels of Aβ42. For MTL, no associations were found after

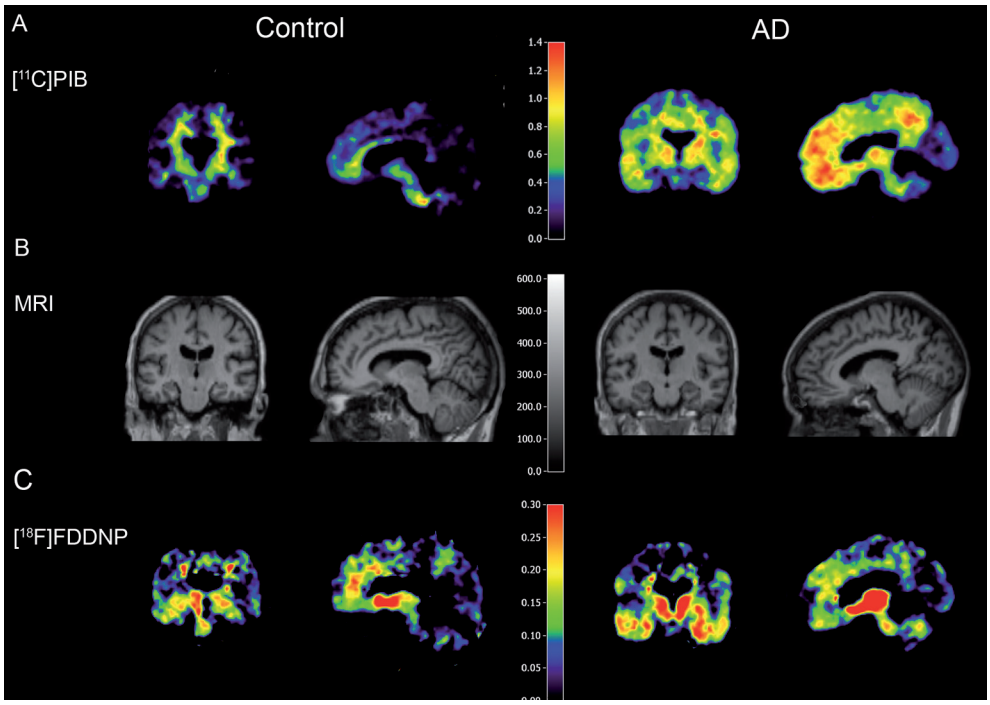

Figure 1: Examples of parametric coronal (left column) and sagittal (right column) [^{11}C]PIB (row A) and [^{18}F]FDDNP (row C) BP_{ND} images in a control subject and an AD patient with their coregistered MRI (row B). [^{11}C]PIB and [^{18}F]FDDNP scans were performed in the same subjects. Corresponding CSF values for the AD patient (60 years) were: Aβ42 = 504 pg/mL; tau = 837 pg/mL. For the healthy control subject (61 years) CSF levels were: Aβ42 = 1123 pg/mL; tau = 245 pg/mL.

Table 2: Pearson's correlation coefficients between CSF biomarkers and tracer BP_{ND}.

	BP_{ND} [^{11}C]PIB		BP_{ND} [^{18}F]FDDNP	
CSF biomarker (pg/mL)	Aβ1–42	Tau	Aβ1–42	Tau
Brain region				
Global	-0.72**	0.58**	-0.37*	0.56**
Frontal	-0.74**	0.58**	-0.37*	0.56**
Medial temporal	-0.36*	0.26	-0.13	0.25
Temporal	-0.71**	0.59**	-0.26	0.45*
Posterior cingulate	-0.69**	0.53*	-0.12	0.33*
Parietal	-0.68**	0.56**	-0.39*	0.48*

Aβ1–42, beta-amyloid; BP_{ND}, binding potential.

*) $p < 0.05$
**) $p \leq 0.001$

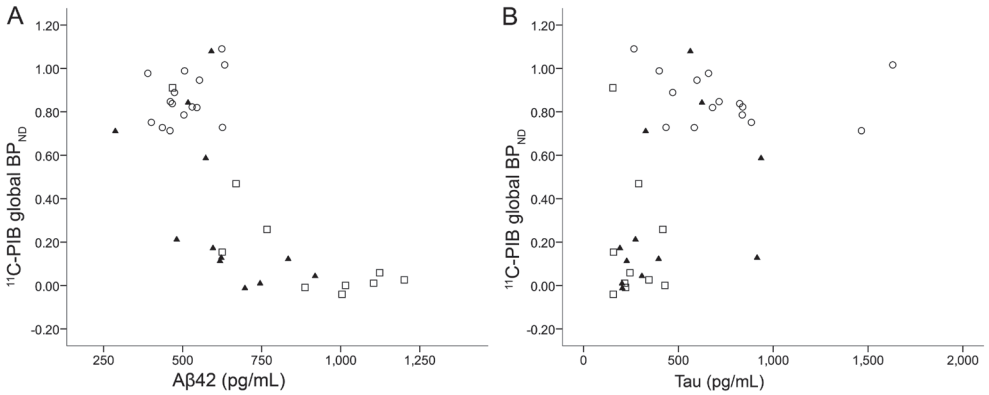

Figure 2: Scatter plots of [^{11}C]PIB binding (global BP$_{ND}$) against CSF levels of (A) Aβ42 and (B) tau. Open circles represent patients with AD, filled triangles patients with MCI and open squares healthy controls. Note, that CSF values are shown as measured, whilst statistical analyses were performed on log-transformed values. Lower CSF levels of Aβ42 (A: r=-0.72, p<0.001) and higher tau levels (B: r=0.58, p<0.001) were associated with higher global [^{11}C]PIB binding.

correcting for grey matter ROI volume, age, sex and diagnosis. Nevertheless, the effect size of the association between CSF tau and [^{18}F]FDDNP binding in this region remained comparable (standardised β=0.33). Results were essentially the same in the third model, where both CSF biomarkers were entered simultaneously (data not shown). Finally, these analyses were repeated after exclusion of the 5 subjects with intervals between LP and PET of more than 12 months. Results remained unaltered for associations with [^{11}C]PIB binding (model 2, global binding; CSF Aβ42: standardised β=-0.50, p<0.01; CSF tau: standardised β=0.19, p=0.29). For [^{18}F]FDDNP, associations with both CSF Aβ42 and tau became even stronger (model 2, global

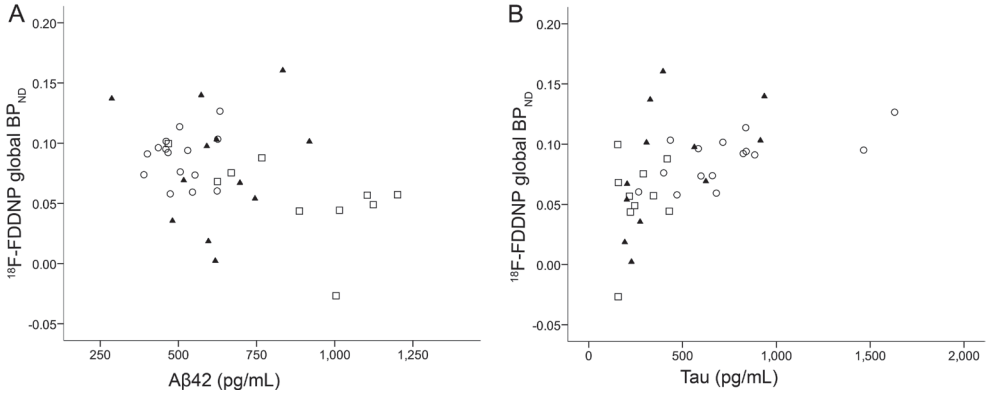

Figure 3: Scatter plots of [^{18}F]FDDNP binding (global BP$_{ND}$) against CSF levels of (A) Aβ42 and (B) tau. Open circles represent patients with AD, filled triangles patients with MCI and open squares healthy controls. Note, that CSF values are shown as measured, whilst statistical analyses were performed on log-transformed values. Lower CSF levels of Aβ42 (A: r=-0.37, p<0.05) and higher tau levels (B: r=0.56, p<0.001) were associated with higher global [^{18}F]FDDNP binding.

Table 3: Linear regression analysis between CSF biomarkers and tracer BP_{ND}.

	Model 1		Model 2	
CSF biomarker (pg/mL)	Aβ42	Tau	Aβ42	Tau
Brain region				
[^{11}C]PIB BP_{ND}				
Global [^{11}C]PIB	-0.72**	0.59**	-0.50**	0.17
Frontal	-0.75**	0.60**	-0.56**	0.18
Medial Temporal	-0.42*	0.37*	-0.15	0.03
Temporal	-0.69 **	0.57 **	-0.46**	0.17
Posterior cingulate	-0.69**	0.52**	-0.47*	0.12
Parietal	-0.67**	0.57**	-0.43*	0.14
[^{18}F]FDDNP BP_{ND}				
Global [^{18}F]FDDNP	-0.36*	0.59**	-0.26	0.62*
Frontal	-0.36*	0.56**	-0.27	0.62*
Medial Temporal	-0.16	0.34+	-0.07	0.33
Temporal	-0.29 +	0.56**	-0.12	0.50*
Posterior cingulate	-0.12	0.33 *	-0.03	0.46*
Parietal	-0.36*	0.49*	-0.33	0.44*

Linear regression analyses were performed to adjust for potential confounders. Model 1: adjusted for ROI volume. Model 2: adjusted for ROI volume, age, sex and diagnosis (using dummy variables). Values are given as standardised β's.
Aβ1–42, beta-amyloid; BP_{ND}, binding potential.
+ p< 0.10; * p< 0.05; ** p≤0.001

binding; CSF tau standardised β=0.70, p<0.01; CSF Aβ42: standardised β=-0.42, p=0.09). Again, results were essentially the same in the third model, where both CSF biomarkers were entered simultaneously (data not shown).

Discussion

In the present study relationships between two CSF biomarkers (Aβ42 and tau) and uptake of two PET amyloid tracers ([^{11}C]PIB and [^{18}F]FDDNP) were investigated. Adjusted for ROI volume, age, sex and diagnosis, increased global [^{11}C]PIB binding was specifically related to low CSF levels of Aβ42. In contrast, increased global [^{18}F]FDDNP binding was associated with high CSF levels of tau. These results add to the converging evidence that both PET tracers measure different elements of the neuropathology underlying AD.

These results confirm and extend those of previous studies in which an inverse (*8,9,12*),*(10)* relationship between CSF Aβ42 and [^{11}C]PIB and no *(8)* or only a modest *(10)* relationship between CSF tau and [^{11}C]PIB was demonstrated. Those earlier studies, however, were performed in groups consisting mainly of healthy controls (*8,9*), MCI patients *(10)* or AD patients *(12)*. In the present study this relationship was extended to the entire spectrum of cognitive decline, providing further support for the notion that [^{11}C]PIB measures amyloid load in the brain.

There have been no reports on associations between [^{18}F]FDDNP binding and CSF data. Whilst it has been previously reported that [^{18}F]FDDNP binds with high affinity to both amyloid plaques and neurofibrillary tangles in vitro *(7)*, considerably lower sensitivity for binding to

amyloid containing structures has been reported recently *(30)*. At present, it is still not clear what the specific signal in AD represents *in vivo*. In the present data a positive association between [^{18}F]FDDNP and CSF tau was observed and, after exclusion of five subjects with long intervals between PET and CSF sampling, a moderate inverse association with CSF levels of Aβ42. These results suggests that increased binding of [^{18}F]FDDNP in AD patients may indeed be due to tangle formation and to some extent to plaques. This is in line with a previous study *(7)* showing [^{18}F]FDDNP autopsy tissue staining to co-localise with conventional histochemistry measures of tangles and plaques.

As mentioned above, after exclusion of the five subjects with long intervals between PET scanning and LP, a moderate inverse association was found between [^{18}F]FDDNP binding and CSF levels of Aβ42, which was not present beforehand. Previously, it was shown that, in case of repeat LP, CSF biomarkers hardly change over time *(29)*. Therefore, these results are unlikely to be caused by changes in CSF. For [^{18}F]FDDNP, an increase in binding over time has been described in subjects with clinical evidence of disease progression *(2)*. Changes in the substrate for [^{18}F]FDDNP binding are therefore more likely to have contributed to these results. Furthermore, exclusion of relative outliers could also have contributed to the stronger association.

In general, for both tracers associations between regional tracer binding and CSF biomarkers were similar as those for global binding, except for MTL, where no associations were found. This finding is remarkable for [^{18}F]FDDNP, as the MTL displayed the highest [^{18}F]FDDNP binding values for all three diagnostic groups. The lack of associations in this region may be due to technical reasons. This region, being the volume weighted average of entorhinal cortex and hippocampus, was relatively small, making it sensitive to noise. Furthermore, as MTL atrophy is commonly seen in AD *(31)*, differences in MTL volumes between diagnostic groups may lead to partial volume effects and thus underestimation of the signal in AD patients. This potentially causes reduced variability in MTL BP_{ND} between diagnostic groups and consequently a lack of association with CSF biomarkers. When linear regression analyses were performed with adjustment for grey matter ROI volume, a trend was found for high CSF levels of tau to be associated with increased [^{18}F]FDDNP binding in the MTL. After additional adjustment for age, sex and diagnosis, this trend disappeared, although the effect size remained strong. This suggests that indeed partial volume effects in the MTL have at least partly underestimated tracer binding in this region. However, PET data were not corrected for partial volume effects. The choice was made not to correct for partial voluming, as potential overcorrection may lead to an artificially high signal. This approach ascertains that any observed increase in binding is real, which is a deliberate conservative approach. But more importantly, current status of partial volume correction (PVC) in amyloid imaging is not clear. For [^{11}C]PIB studies, several PVC methods have been used, most commonly a method developed by Meltzer *(32)* and an algorithm implemented in the PMOD software package (PMOD Technologies Ltd., Adliswil, Switzerland). These methods are based on T1-weighted structural MR scans. However, a study performed by our group *(33)* showed that accuracy of MR based PVC depends greatly on MR scanner type, scanning sequence and gray/white matter segmentation algorithm. The results

of that study indicate that accuracy of PVC should be further evaluated before it can be used in patient studies.' The main strength of the present study is its unique design, performing CSF sampling and PET scanning with both ligands in the same subjects along the spectrum of cognitive decline. This enabled a direct assessment of the relationship between two types of biomarkers both aimed at identifying underlying AD pathology. Further research in tauopathies other than AD will be valuable in gaining more insight in the validity of [^{18}F]FDDNP for *in vivo* imaging of tau pathology. In addition, longitudinal studies are needed to investigate possible increases in [^{18}F]FDDNP binding over time.

Acknowledgements

This work was financially supported by the Internationale Stichting Alzheimer Onderzoek (ISAO, grant 05512), and the American Health Assistance Foundation (AHAF, grant A2005-026). The clinical database structure was developed with funding from Stichting Dioraphte. We would like to thank Anke A. Dijkstra for help with the data analysis, the PET radiochemistry and technology staff of the Division of Nuclear Medicine & PET Research for tracer production and acquisition of PET data, and the technology staff of the Department of Radiology for acquisition of the MRI data.

References

1. Klunk WE, Engler H, Nordberg A et al. Imaging brain amyloid in Alzheimer's disease with Pittsburgh Compound-B. *Ann Neurol* 2004;55:306-319.
2. Small GW, Kepe V, Ercoli LM et al. PET of brain amyloid and tau in mild cognitive impairment. *N Engl J Med* 2006;355:2652-2663.
3. Blennow K, Hampel H. CSF markers for incipient Alzheimer's disease. *Lancet Neurol* 2003;2:605-613.
4. Klunk WE, Lopresti BJ, Ikonomovic MD et al. Binding of the positron emission tomography tracer Pittsburgh compound-B reflects the amount of amyloid-beta in Alzheimer's disease brain but not in transgenic mouse brain. *J Neurosci* 2005;25:10598-10606.
5. Klunk WE, Wang Y, Huang GF et al. The binding of 2-(4'-methylaminophenyl)benzothiazole to postmortem brain homogenates is dominated by the amyloid component. *J Neurosci* 2003;23:2086-2092.
6. Ikonomovic MD, Klunk WE, Abrahamson EE et al. Post-mortem correlates of in vivo PiB-PET amyloid imaging in a typical case of Alzheimer's disease. *Brain* 2008;131:1630-1645.
7. Agdeppa ED, Kepe V, Liu J et al. Binding characteristics of radiofluorinated 6-dialkylamino-2-naphthylethylidene derivatives as positron emission tomography imaging probes for beta-amyloid plaques in Alzheimer's disease. *J Neurosci* 2001;21:RC189.
8. Fagan AM, Mintun MA, Mach RH et al. Inverse relation between in vivo amyloid imaging load and cerebrospinal fluid Abeta42 in humans. *Ann Neurol* 2006;59:512-519.
9. Fagan AM, Roe CM, Xiong C et al. Cerebrospinal fluid tau/beta-amyloid(42) ratio as a prediction of cognitive decline in nondemented older adults. *Arch Neurol* 2007;64:343-349.
10. Forsberg A, Engler H, Almkvist O et al. PET imaging of amyloid deposition in patients with mild cognitive impairment. *Neurobiol Aging* 2008;29:1456-1465.
11. Koivunen J, Pirttila T, Kemppainen N et al. PET Amyloid Ligand [C]PIB Uptake and Cerebrospinal Fluid beta-Amyloid in Mild Cognitive Impairment. *Dement Geriatr Cogn Disord* 2008;26:378-383.
12. Grimmer T, Riemenschneider M, Forstl H et al. Beta Amyloid in Alzheimer's Disease: Increased Deposition in Brain Is Reflected in Reduced Concentration in Cerebrospinal Fluid. *Biol Psychiatry* 2009.
13. Tolboom N, Yaqub M, van der Flier WM et al. Detection of Alzheimer pathology *in vivo* using both [^{11}C]PIB and [^{18}F]FDDNP positron emission tomography. *J Nucl Med* 2009;50:191-197.
14. McKhann G, Drachman D, Folstein M et al. Clinical diagnosis of Alzheimer's disease: report of the NINCDS-ADRDA Work Group under the auspices of Department of Health and Human Services Task Force on Alzheimer's Disease. *Neurology* 1984;34:939-944.
15. Petersen RC, Smith GE, Waring SC et al. Mild cognitive impairment: clinical characterization and outcome. *Arch Neurol* 1999;56:303-308.
16. Agdeppa ED, Kepe V, Petri A et al. In vitro detection of (S)-naproxen and ibuprofen binding to plaques in the Alzheimer's brain using the positron emission tomography molecular imaging probe 2-(1-[6-[(2-[(18)F]fluoroethyl)(methyl)amino]-2-naphthyl]ethylidene)malono nitrile. *Neuroscience* 2003;117:723-730.
17. Brix G, Zaers J, Adam LE et al. Performance evaluation of a whole-body PET scanner using the NEMA protocol. National Electrical Manufacturers Association. *J Nucl Med* 1997;38:1614-1623.
18. Tolboom N, Yaqub M, Boellaard R et al. Test-retest variability of quantitative [11C]PIB studies in Alzheimer's Disease. *Eur J Nucl Med* 2009;36:1629-38.
19. Wilson AA, Garcia A., Chestakova A., Kung H.F., Houle S. A rapid one-step radiosynthesis of the beta-amyloid imaging radiotracer N-methyl-[C-11]2-('4-methylaminophenyl)-6-hydroxybenzothiazole ([C-11]-6-OH-BTA-1).. *Journal of labelled compounds and radiopharmaceuticals* 2004;47:679-682.
20. Klok RP, Klein PJ, van Berckel BN et al. Synthesis of 2-(1,1-dicyanopropen-2-yl)-6-(2-[18F]-fluoroethyl)-methylamino-naphthalene ([18F] FDDNP). *Appl Radiat Isot* 2008;66:203-207.
21. Maes F, Collignon A, Vandermeulen D, Marchal G, Suetens P. Multimodality image registration by maximization of mutual information. *IEEE Trans Med Imaging* 1997;16:187-198.
22. Svarer C, Madsen K, Hasselbalch SG et al. MR-based automatic delineation of volumes of interest in human brain PET images using probability maps. *Neuroimage* 2005;24:969-979.

23. Wu Y, Carson RE. Noise reduction in the simplified reference tissue model for neuroreceptor functional imaging. *J Cereb Blood Flow Metab* 2002;22:1440-1452.
24. Yaqub M, Tolboom N, Boellaard R et al. Simplified parametric methods for [11C]PIB studies. *Neuroimage* 2008;42:76-86.
25. Yaqub M, Boellaard R, van Berckel BNM et al. Evaluation of tracer kinetic models for analysis of [^{18}F] FDDNP studies. *Mol Imaging Biol 2009;11:322-33.*
26. Innis RB, Cunningham VJ, Delforge J et al. Consensus nomenclature for in vivo imaging of reversibly binding radioligands. *J Cereb Blood Flow Metab* 2007;27:1533-1539.
27. Yamaguchi H, Hirai S, Morimatsu M, Shoji M, Nakazato Y. Diffuse type of senile plaques in the cerebellum of Alzheimer-type dementia demonstrated by beta protein immunostain. *Acta Neuropathol* 1989;77:314-319.
28. Joachim CL, Morris JH, Selkoe DJ. Diffuse senile plaques occur commonly in the cerebellum in Alzheimer's disease. *Am J Pathol* 1989;135:309-319.
29. Bouwman FH, van der Flier WM, Schoonenboom NS et al. Longitudinal changes of CSF biomarkers in memory clinic patients. *Neurology* 2007;69:1006-1011.
30. Thompson PW, Ye L, Morgenstern JL et al. Interaction of the amyloid imaging tracer FDDNP with hallmark Alzheimer's disease pathologies. *J Neurochem* 2009.
31. de Leon MJ, Convit A, George AE et al. In vivo structural studies of the hippocampus in normal aging and in incipient Alzheimer's disease. *Ann N Y Acad Sci* 1996;777:1-13.
32. Meltzer CC, Leal JP, Mayberg HS, Wagner HN, Jr., Frost JJ. Correction of PET data for partial volume effects in human cerebral cortex by MR imaging. *J Comput Assist Tomogr* 1990;14:561-570.
33. Kloet RW, van Berckel BNM, Pauwels PJW et al. Effects of MR scanner type, scanning sequence and segmentation algorithm on MR-based partial volume corrections of [^{11}C](*R*)-PK11195 studies. *Neuroimage* 2006;31:T83.